

Fast interpolation of beampatterns for partially-occluded and time-variant facets using a Fourier domain warping method

A.J. Hunter and M.P. Hayes

Electrical and Computer Engineering Department, University of Canterbury,
Private Bag 4800, Christchurch, New Zealand.

Email: {a.hunter,m.hayes}@elec.canterbury.ac.nz

Abstract

This paper presents a new technique for the rapid computation of the beampattern for the field scattered from a facet. We show how an affine transform and application of the warping property of the Fourier transform can be used to calculate the beampattern of an arbitrary triangular facet from the beampattern of a unit right-angle triangular facet. Thus only a single Fourier transform needs to be calculated and stored; this is then interpolated as required. When a facet is partially occluded we describe how the visible region of the facet can be partitioned into a number of smaller triangular facets, which can be evaluated using the new technique.

Keywords: synthetic aperture sonar/radar, coherent scattering, occlusion, facet beampatterns

1 Introduction

The simulation of coherent imagery from arbitrary scenes, say for synthetic aperture radar or sonar, is computationally intensive. This is because it requires a numerical integration of the Kirchhoff integral [1] over each elemental region in the scene. Moreover, the computation is complicated by multiple scattering, occlusion, and diffraction of the scattered field.

One approach to reduce the computation is to divide the scene into a number of facets; each sufficiently small so that the observation point of the scattered field is in the far-field of each facet. This allows the application of the Fraunhofer approximation so that the Kirchhoff integral for the facet can be simplified by a Fourier transform [1]. This Fourier transform is often called the facet beampattern. Since it only depends on the shape of the facet it can be precomputed and then interpolated for each observation point [2, 3].

While this facet beampattern approach greatly reduces the complexity of the numerical integration, it requires a beampattern to be computed and stored for each facet. In this paper we present a new technique where only a single beampattern needs to be calculated and stored; that for a unit right-angle triangular facet. The beampattern for an arbitrary triangular facet is then found using an affine transform and application of the warping property of the Fourier transform.

We start in Section 2 by looking at facet beampatterns, in particular the beampattern of a triangular facet. We then show in Section 3 how the response for an arbitrary triangular facet can be determined using affine transformations coupled with Fourier warping. This technique is then applied in Section 4 to determine the response of a partially occluded facet. We then discuss in Section 6 how this warping can be applied to deal with time variant facets and temporal Doppler effects.

2 Facet beampatterns

The beampattern of a facet describes the angular dependence of the scattering from a smooth facet. If the observation point is in the far-field of the aperture (Fraunhofer approximation) the beampattern is related to the Fourier transform of the aperture function [2]. The beampattern can also be applied to determine the diffuse component of the field scattered from a rough surface [2].

2.1 Triangular facet

The triangular facet is an important case since any surface can be tessellated into a continuous collection of triangular facets [4]. A unit right-angle triangular facet is illustrated in Figure 1. This has an aperture function described by

$$a(x, y) = \text{rect}\left(x + \frac{1}{6}\right) \text{rect}\left(y + \frac{1}{6}\right) \text{rect}\left(\frac{x+y}{2}\right), \quad (1)$$

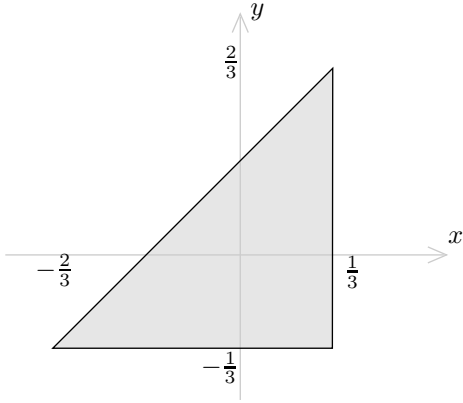


Figure 1: The unit right-angle triangle centred about its centroid.

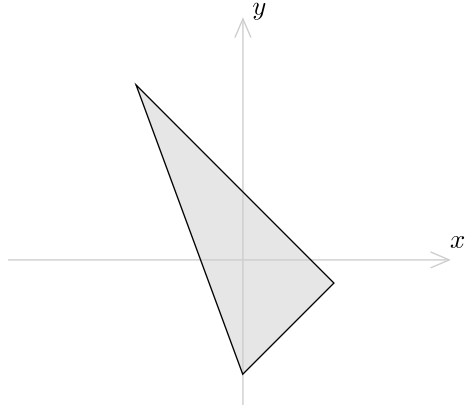


Figure 3: An arbitrary triangle centred about its centroid.

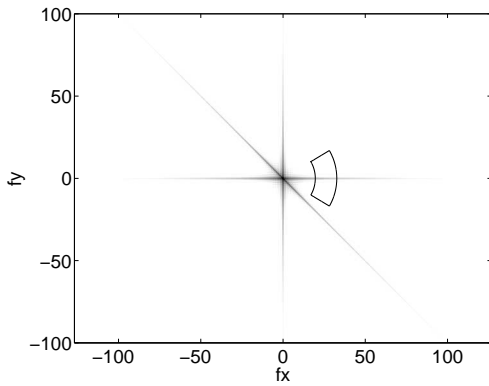


Figure 2: The 2-D Fourier transform of the unit right-angle triangle. The boxed region indicates the spatial frequencies required for the trajectory of the imaging platform and the temporal bandwidth.

with a corresponding 2-D Fourier transform given by

$$A(f_x, f_y) = \frac{j}{2\pi f_x} \exp\left(j\pi\left(\frac{1}{3}f_x + \frac{1}{3}f_y\right)\right) \times \left[\exp(-j\pi f_x) \operatorname{sinc}(f_y) - \operatorname{sinc}(f_x + f_y)\right]. \quad (2)$$

The response of this facet is shown in Figure 2 for spatial frequencies f_x and f_y .

3 Fourier domain warping

In this section an efficient method for generating beam patterns for arbitrary triangular facets is introduced. The method uses the *warping* property of the Fourier transform.

The warping property of the Fourier transform states that warping in one domain results in an inverse warping in the other domain; this is a

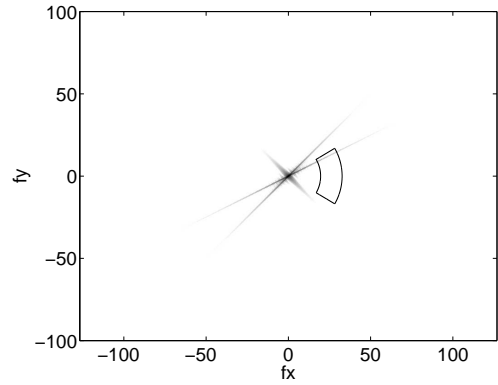


Figure 4: The 2-D Fourier transform of the triangle in Figure 3. The boxed area indicates the region of interpolated points.

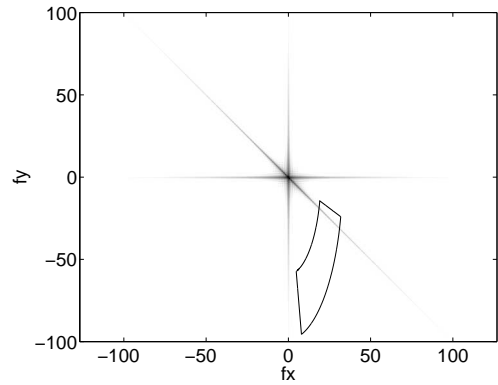


Figure 5: The 2-D Fourier transform of the unit right-angle triangle. This is interpolated at points (indicated by the boxed region) that have been warped using the inverse of the affine transform that is required to warp the unit triangle to the arbitrary triangle.

generalisation of the scaling and shifting properties of the Fourier transform [5]. For example, consider

the Fourier transform pair

$$a(\mathbf{x}) \longleftrightarrow A(\mathbf{f}_x), \quad (3)$$

where $a(\mathbf{x})$ denotes the aperture function of a facet and $A(\mathbf{f}_x)$ denotes its beampattern evaluated at spatial frequencies \mathbf{f}_x . By the warping property of the Fourier transform,

$$a(\mathbf{R}\mathbf{x}) \longleftrightarrow \frac{1}{\det(\mathbf{R})} A(\mathbf{R}^{-1}\mathbf{f}_x), \quad (4)$$

where \mathbf{R} is a matrix that describes the transformation of a point \mathbf{x} to a point $\mathbf{x}' = \mathbf{R}\mathbf{x}$ and $\det(\mathbf{R})$ is the determinant of \mathbf{R} .

The response from a facet is calculated by evaluating the Fourier transform of the facet at spatial frequencies determined by the imaging geometry [2]. Alternatively the Fourier transform of the right-angle triangle can be evaluated using spatial frequencies warped by the matrix \mathbf{R}^{-1} as shown in (4). The matrix \mathbf{R} describes an affine transformation that warps the arbitrary triangle to the unit right-angle triangle. The advantage of this approach is that the Fourier transform of each unique facet does not need to be determined. This is illustrated in Figures 3 to 5 where the region of interpolated points is for a SAS imaging geometry.

3.1 Affine transformation

The Fourier transform of an arbitrary triangular facet can be determined from (2) using the warping property of the Fourier transform; an arbitrary triangle can be transformed, or warped, to the unit right-angle triangle and the Fourier relationship can be used to determine the Fourier transform of the warped facet.

A triangle is defined by its three vertices: \mathbf{x}_0 , \mathbf{x}_1 , and \mathbf{x}_2 . These vectors can be combined to create a matrix $\mathbf{T} = (\mathbf{x}_0, \mathbf{x}_1, \mathbf{x}_2)$, i.e.,

$$\mathbf{T} = \begin{pmatrix} x_0 & x_1 & x_2 \\ y_0 & y_1 & y_2 \\ z_0 & z_1 & z_2 \end{pmatrix}, \quad (5)$$

where $\mathbf{x}_0 = (x_0, y_0, z_0)$, etc. Similarly, the unit right-angle triangle can be described by the matrix

$$\mathbf{T}_u = \begin{pmatrix} \frac{1}{3} & \frac{1}{3} & -\frac{2}{3} \\ -\frac{1}{3} & \frac{2}{3} & -\frac{1}{3} \\ 0 & 0 & 0 \end{pmatrix}. \quad (6)$$

The matrix describing an arbitrary triangle can be warped into the matrix describing the unit right-angle triangle using an affine transformation, i.e.,

$$\mathbf{T} = \mathbf{R} \mathbf{T}_u, \quad (7)$$

where \mathbf{T} and \mathbf{T}_u are assumed to be centred at the origin. The matrix \mathbf{R} is often termed the rotation matrix but it describes a more general transformation than a simple rotation; it can describe rotation, shear, and scaling.

The rotation matrix required to transform \mathbf{T} to \mathbf{T}_u can be determined from (7) using

$$\mathbf{R} = \mathbf{T} (\mathbf{T}_u^T \mathbf{T}_u)^{-1} \mathbf{T}_u^T, \quad (8)$$

where the superscript \cdot^T denotes the matrix transpose operation and $(\mathbf{T}_u^T \mathbf{T}_u)^{-1} \mathbf{T}_u^T$ is the pseudo-inverse of \mathbf{T}_u .

3.2 Non-triangular facets

The beampattern of a non-triangular facet can be determined by partitioning it into a number of triangular facets and using the Fourier linearity theorem to sum the beampatterns for each triangular facet to get the overall facet beampattern.

For example, the aperture function of a quadrilateral is the combination of two triangular aperture functions:

$$a_Q(\mathbf{x}) = a_{T_1}(\mathbf{x} - \mathbf{x}_1) + a_{T_2}(\mathbf{x} - \mathbf{x}_2). \quad (9)$$

Here a_{T_1} and a_{T_2} are assumed to have centroids at the origin and \mathbf{x}_1 and \mathbf{x}_2 are translation vectors. Using the Fourier linearity and shift theorems, the combined beampattern is the superposition of the beampatterns for the two triangular apertures appropriately phase shifted:

$$A_Q(\mathbf{f}_x) = A_{T_1}(\mathbf{f}_x) \exp(-j2\pi\mathbf{f}_x \cdot \mathbf{x}_1) + A_{T_2}(\mathbf{f}_x) \exp(-j2\pi\mathbf{f}_x \cdot \mathbf{x}_2). \quad (10)$$

The two triangular apertures can be mapped to a standard right angle triangle using two affine transformations:

$$a_{T_1}(\mathbf{x}) = a_{T_u}(\mathbf{R}_1\mathbf{x}), \quad (11)$$

$$a_{T_2}(\mathbf{x}) = a_{T_u}(\mathbf{R}_2\mathbf{x}), \quad (12)$$

where the rotation matrices are calculated using (8). Thus using (10) and (4) the composite beampattern is

$$A_Q(\mathbf{f}_x) = \frac{A_{T_u}(\mathbf{R}_1^{-1}\mathbf{f}_x)}{\det(\mathbf{R}_1)} \exp(-j2\pi\mathbf{f}_x \cdot \mathbf{x}_1) + \frac{A_{T_u}(\mathbf{R}_2^{-1}\mathbf{f}_x)}{\det(\mathbf{R}_2)} \exp(-j2\pi\mathbf{f}_x \cdot \mathbf{x}_2). \quad (13)$$

In general, the composite beampattern for N triangular facets is

$$A(\mathbf{f}_x) = \sum_{n=1}^N \frac{A_{T_u}(\mathbf{R}_n^{-1}\mathbf{f}_x)}{\det(\mathbf{R}_n)} \exp(-j2\pi\mathbf{f}_x \cdot \mathbf{x}_n), \quad (14)$$

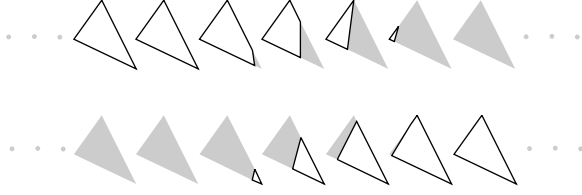


Figure 6: Demonstration of how the effective shape of a facet changes due to occlusion as the observation point changes.

where x_n and \mathbf{R}_n are the translation vector and rotation matrix for the n^{th} facet.

4 Beampatterns of partially occluded facets

When a facet is in the shadow region of another facet it is said to be occluded. If it is completely occluded it does not contribute to the total field and can be ignored. However, when it is partially occluded, its beampattern changes since its effective shape has changed. Moreover, as the observation (and illumination) points are changed, the shadows move and thus the effective shape changes. This is illustrated in Figure 6.

The most common occlusion is a first-order shadow where a linear shadow is cast across the facet. For a triangular facet this results in an effective facet that is a triangle or quadrilateral shape. To find the visible region of a triangular facet occluded by a simple linear shadow we employ an iterative ray-tracing approach as shown in Figure 7. Here rays are traced to the corners of the facet to find the visible vertices. Then additional rays are traced for each partly occluded edge using a bisection search.

The beampattern of a quadrilateral facet can be computed by partitioning the quadrilateral into two triangles (see Figure 8) and summing the responses using the method described in Section 3.2. Higher order shadows are processed in a similar manner by partitioning the visible portion of the facet into more triangular facets.

5 Results

To illustrate the modelling of a partially occluded facet using the Fourier domain warping method we use a Synthetic Aperture Sonar (SAS) example. The scene (shown in Figure 9) consists of a $1 \times 1\text{m}$ triangular facet partially occluded by a 1m diameter sphere for portions of the sonar tow-path.

A naive approach is to model the occlusion using a binary shadow mask where a ray is traced to the facet centroid to determine if the facet is occluded. The binary mask is shown in Figure 10 for

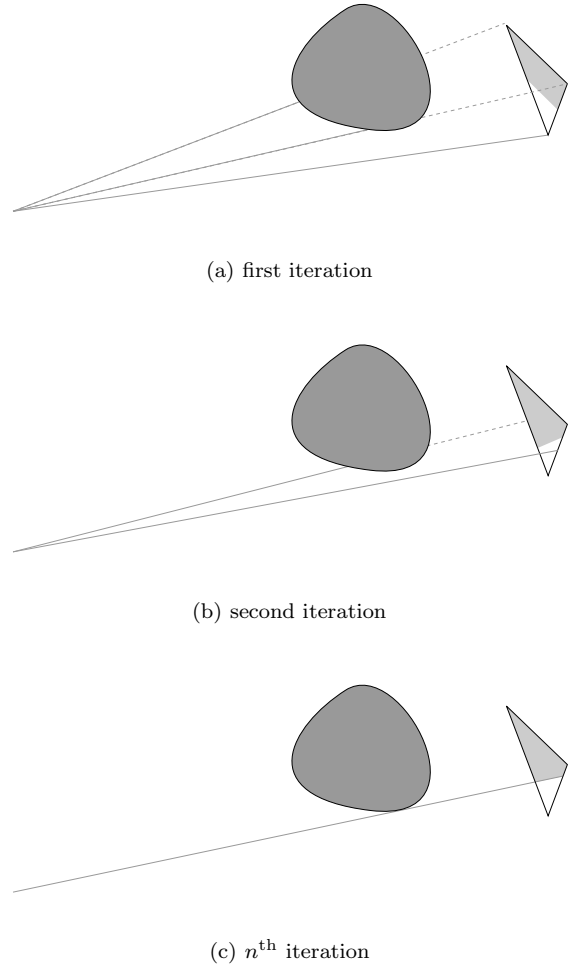


Figure 7: Iterative determination of first-order shadows.

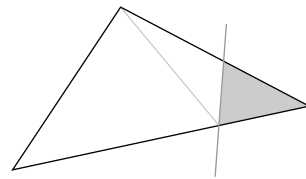


Figure 8: A facet occluded by a first-order shadow yields an effective facet that is a triangle or quadrilateral shape. A quadrilateral can be partitioned into two triangles.

the example scene. Figure 11(a) shows the SAS imagery of the non-occluded facet that is rotated by 10 deg with respect to the tow-path. Here the dominant scattering points are the three corners of the triangle and the binary shadow mask is valid since the corners have small extent. Figure 11(b) shows the imagery of the occluded triangle using a binary mask. The along-track blurring is caused

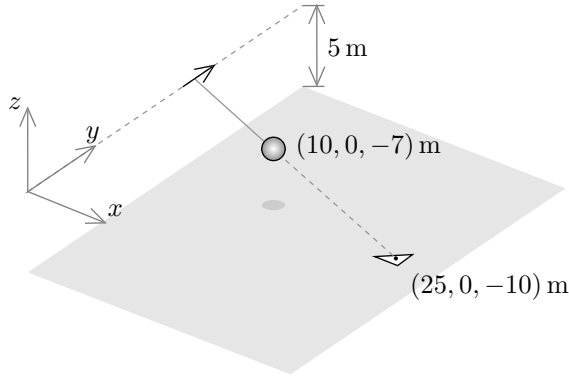


Figure 9: The example scene consists of a 1×1 m triangular facet that is partially occluded by a 1m diameter sphere.

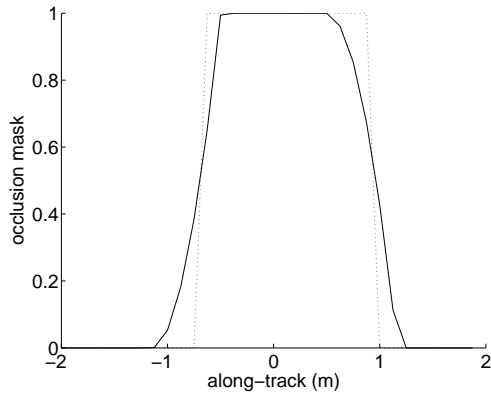
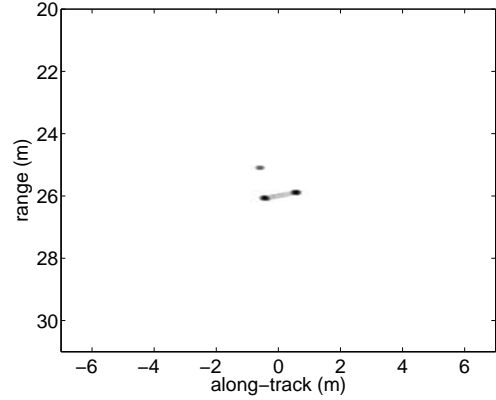


Figure 10: The masks used to determine the scattering magnitude. The dotted line is a simple binary mask using a single ray traced to the facet centroid. The solid line is a mask using the area of the effective facet.

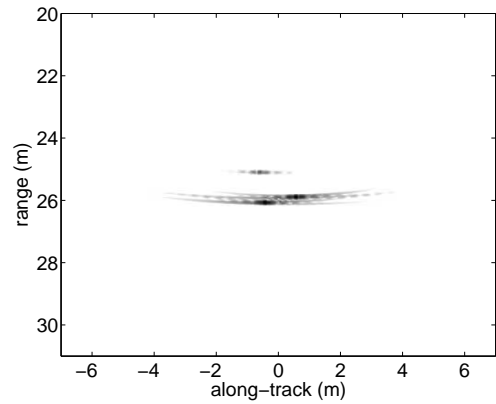
by the resolution loss due to the reduced synthetic aperture.

When the edge of the triangle is aligned with the tow-path the dominant scattering points are along the triangle edge. Here a simple binary mask does not suffice. The imagery of the non-occluded facet is shown in Figure 12(a) and the imagery obtained using the binary mask is shown in Figure 12(b) where significant along-track blurring artefacts have been introduced.

Using the Fourier domain warping method the triangle is partitioned into two triangles, warped to match the effective facet that is determined using the first-order iterative approach. The resultant imagery is shown in Figure 12(c). The along-track blurring has been reduced and is comparable to the results in Figure 11(b).



(a) no shadow



(b) binary mask

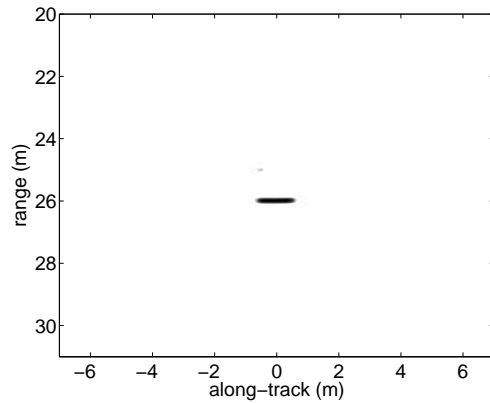
Figure 11: SAS imagery of a triangle facet. The triangle edge is rotated 10 deg with respect to the tow-path. Figure (a) shows the imagery of the non-occluded facet and Figure (b) shows the imagery using a binary shadow mask.

6 Discussion

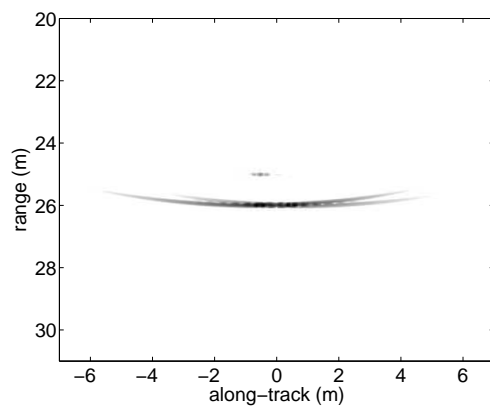
The beampattern warping approach presented here can also be applied to calculate moving beampatterns of time-variant facets; say for example the surface of the ocean. The warping is a simple affine transform of the lookup coordinates for mapping arbitrary triangles to a unit right angle triangle with a precomputed Fourier transform.

Another application for beampattern warping is to model temporal Doppler where there is relative movement between the scene and observation and/or illumination points. Here the warping is applied to the temporal frequency domain instead of the spatial frequency domain.

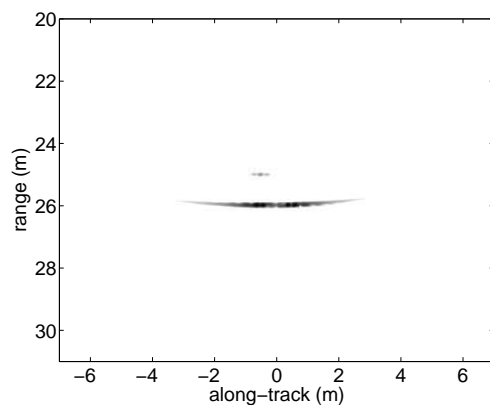
The warping approach becomes more difficult when the facets are shadowed by more complicated



(a) no shadow



(b) binary mask



(c) warping method

Figure 12: SAS imagery of a triangle facet. The triangle edge is aligned with the tow-path. Figure(a) shows the imagery of the non-occluded facet, Figure (b) shows the imagery using a binary shadow mask, and Figure(c) shows the imagery using the Fourier domain warping method.

shapes. One strategy is to subdivide the occluded facet into many smaller facets so that the shadows become simpler and that the integration errors become smaller.

In this paper we have ignored diffraction effects, where the incident field and/or scattered field is diffracted around objects causing blurring of shadow boundaries. This can be modelled using the geometric theory of diffraction but requires more computation since the shadow boundaries are no longer sharp.

7 Conclusions

In this paper we have shown how the simulation of coherent imagery from arbitrary scenes can be more efficiently computed. The key is to warp the facets comprising the scene using an affine transform into a standard triangular facet. The beam-pattern of this standard facet can be precomputed using a 2-D Fourier transform. This beam-pattern is then interpolated at spatial frequencies transformed by an inverse warping.

The beam-pattern warping method can also be used for efficient modelling of time-variant facets, shadowed facets, and temporal Doppler effects.

Acknowledgements

The authors thank Hayden Callow for his useful discussions. Alan Hunter thanks the University of Canterbury for his Doctoral Scholarship.

References

- [1] J. W. Goodman, *Fourier Optics*. New York: M^cGraw-Hill, 1968.
- [2] A. J. Hunter, M. P. Hayes, and P. T. Gough, "Simulation of multiple-receiver, broadband interferometric SAS imagery," in *Oceans 2003*, (San Diego, USA), IEEE/MTS, September 2003. CDROM.
- [3] A. J. Hunter and M. P. Hayes, "A distributed acoustic renderer for SAS image simulation," in *IVCNZ2004, Image and Vision Computing New Zealand*, (Akaroa, New Zealand), pp. 333–338, 22–23 November 2004.
- [4] J. D. Foley, A. van Dam, S. K. Feiner, and J. F. Hughes, *Computer Graphics: Principles and Practice*. Addison-Wesley, 2 ed., 1997.
- [5] R. N. Bracewell, *The Fourier Transform and its Applications*. New York: M^cGraw-Hill, 1978.